An IC Piezoresistive Pressure Sensor for Biomedical Instrumentation

SAMAUN, KENSALL D WISE, AND JAMES. B. ANGELL

(NASA-CR-142604) AN I C PIEZORESISTIVE PRESSURE SENSOR FOR BIOMEDICAL INSTRUMENTATION (Stanford Univ.) 10 p

N75-72914

Unclas
00/98 14639

Reprinted by permission from IEEE TRANSACTIONS ON BIOMEDICAL ENGINEERING

Vol BME-20, No. 2, March 1973, pp 101 109
Copyright 1973, by the Institute of Electrical and Electronic Engineers, Inc
PRINTED IN THE U.S.A

Reprinted by permission from IEEE TRANSACTIONS ON BIOMEDICAL ENGINEERING

Vol BME-20, No. 2, March 1973, pp 101–109
Copyright 1973, by the Institute of Electrical and Electronic Engineers, Inc.
PRINTED IN THE U.S.A

An IC Piezoresistive Pressure Sensor for Biomedical Instrumentation

SAMAUN, KENSALL D. WISE, AND JAMES B. ANGELL

Abstract–A thin-diaphragm piezoresistive pressure sensor for biomedical instrumentation has been developed using monolithic integrated circuit (IC) techniques. The piezoresistive effect has been chosen for this device because it provides an observable resistance change that is a linear function of pressure and is observable at low stress levels. *A* diaphragm is used as a stress magnifying device; its magnification is proportional to the square of the ratio of the diaphragm diameter to its thickness. The pressure-induced stresses in the diaphragm are sensed by properly oriented piezoresistors interconnected to form a bridge.

An anisotropic etching technique is used for the formation of the diaphragms; this technique makes possible a novel thickness monitoring scheme that also acts as a chip separation etch. Sensors with diaphragm diameters of 0.5 mm and thickness of only 5 pm, surrounded by a 0.15-mm wide ring of thick silicon, have been batch fabricated using this technique. An intrinsic sensitivity of 14 μV/V supply/mmHg has been achieved.

Temperature drift in these sensors is dominated by the temperature dependence of the piezoresistive coefficient. *A* temperature-compensation circuit has been devised for these sensors by deriving a temperature-dependent signal that is pressure independent for the compensation of the temperature-dependent part of the bridge unbalance voltage.

These sensors, after being mounted on the tip of a small catheter, can be inserted into the biological system through the inner bore of a larger catheter that was formerly occupied by a guide wire. The sensors have been utilized for acute measurements of blood pressure in dogs with satisfactory results.

Manuscript received November 1 1971 revised February 4, 1972 and May 30. 1972 This work was supported by the National Aeronautics and Space Administration under Grant NGR-05-020-401

Samaun was with the Department of Electrical Engineering. Stanford University, Stanford. Calif 94305 He is now with the Department of Electrical Engineering, Bandung Institute of Technology Bandung, Indonesia.

K. D. Wise and J B Angell are with the Department of Electrical Engineering, Stanford University Stanford. Calif 94305

INTRODUCTION

THE MOST COMMON technique for obtaining reliable pressure measurements in biological systems utilizes a flexible stainless steel guide wire about 1 mm in diameter that is inserted into the artery This guide wire is pushed to the desired location under fluoroscopic monitoring, used as a

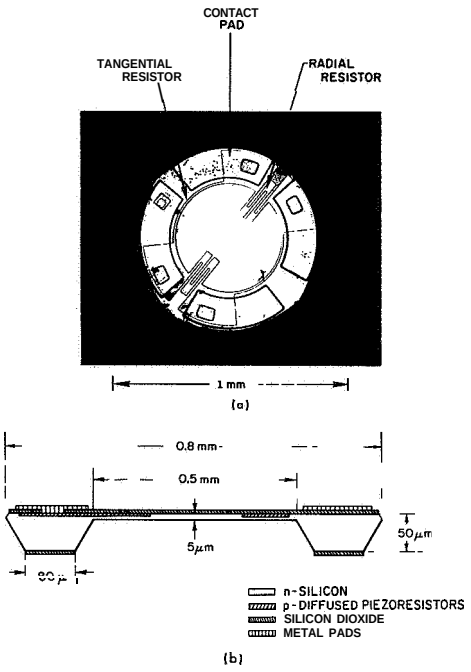

Fig. 1 (a) Top view of **the piezoresistive pressure sensor (b) Cross section** of **the sensor**

guide for insertion of a hollow catheter, and is then removed Finally, the catheter is filled with a suitable fluid whose pressure, a function of the propagation characteristics of the hollow catheter, can depart appreciably from the true *in vivo* pressure.

The object of our research has been to investigate the possibility of fabricating miniature pressure sensors that can substitute for the normal guide wire so that pressures can be measured free of propagation distortion. These transducers, as designed, combine a silicon diaphragm (which serves as a stress magnifying device) with diffused piezoresistors (for sensing the pressure-induced stresses in the diaphragm). Diaphragm thicknesses of about 5 μm are required for obtaining reasonable sensitivities ($\sim$diameter^2/thickness^2) for diameters of about 0.5 mm. **A** supporting nm of thick silicon is then necessary to facilitate the handling and mounting of these structures. Fig. 1(a) shows a photograph of a pressure sensor, Fig. 1(b) shows the cross section.

The diaphragms are formed by etching the silicon wafers using a potassium hydroxide (KOH) anisotropic etch that is inexpensive, easy to handle, and produces flat diaphragms. With KOH, selective etching is easily accomplished using silicon dioxide **as** an etch mask. **A** unique diaphragm thickness monitoring scheme is utilized that also acts as a chip separation etch. Using this technique **as** a final processing step, batch fabrication of the circular pressure-sensitive chips can be realized using standard integrated-circuit **(IC)** processing techniques

The pressure-induced stresses on the diaphragm are sensed by four properly oriented piezoresistors interconnected to form a bridge. Temperature-induced stresses on the diaphragm are compensated for by an external active circuit by extracting a temperature-dependent signal that is pressure independent

The mounting of the small pressure-sensitive chips at the tip of a catheter is an integral part of the transducer development. Since most of the contact between the transducer and the biomedical system is through the packaging, a dominant consideration is the toxicity of the materials used Our present mounting method involves the use of a quartz tube for holding four insulated copper wires together, which are then soldered to the four contact pads on the chip. Sealing of the space between the chip and the quartz tube is done by using epoxy The overall diameter of the finished catheter-tip-mounted sensor is 0.9 mm, which is smaller than the diameter of a conventional guide wire

In the following sections of this paper, the design of these pressure sensors is first discussed in terms of diaphragm stress patterns and crystallographic orientation of the piezoresistors. The fabrication techniques used are then described, and the characteristics of the sensors *in vitro* and *in vivo* are examined.

Design Considerations

Silicon has been used for intravascular biomedical sensors for a number of years. Although no piezoelectric effect is observable in silicon, there are other pressure-sensitive effects that can be utilized for making pressure transducers, such as strain-induced changes in the electrical properties of p-n junctions [1] and the piezoresistive effect [2] Because the piezojunction effect is a bandgap effect, it is observable only at high stress levels, near the fracture stress of silicon. The piezoresistive effect, on the other hand, is observable at low stress levels and is the result of the change in carrier mobility with stress. Combined with the advanced state of silicon-processing technology developed for making **IC's,** this effect makes silicon a desirable material for miniature pressure transducers

To produce observable effects with small pressures, some kind of pressure magnification scheme must be utilized Nearly all sensors that utilize the piezojunction effect employ some sort of stylus arrangement to achieve pressure magnification By concentrating the force on a small area at the point of a needle, large stresses can be generated on a small area Another method utilizes a cantilever beam structure in which the stress-sensitive devices are formed on one side of the beam, one end of which is clamped into a rigid supporting structure Force is applied at the other end of the beam.

The third method, which utilizes a diaphragm structure, seems to be the most desirable for our requirements. **A** circular diaphragm is easily mounted on the tip of a catheter Large pressure magnification can be achieved if large ratios between the diaphragm diameter and its thickness can be realized Piezoresistors can be diffused directly into the high-stress regions of the diaphragm, and miniaturization can be easily achieved using normal **IC** processing.

Stress Pattern and Orientation of the Piezoresistors

Using the theory of plates and shells [3], the radial (σ_r) and tangential (σ_t) stress on the back side of the diaphragm can be related to the applied pressure from the front q, the diaphragm thickness h, the diaphragm radius a, Poisson's ratio ν, and the

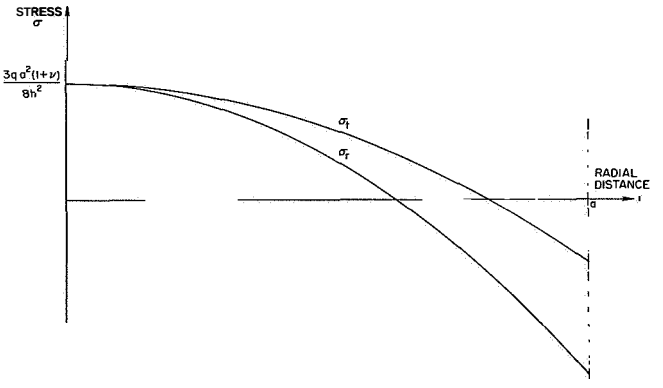

Fig. 2 Radial and tangential stresses on **the back side of a diaphragm due to an applied pressure from the front.**

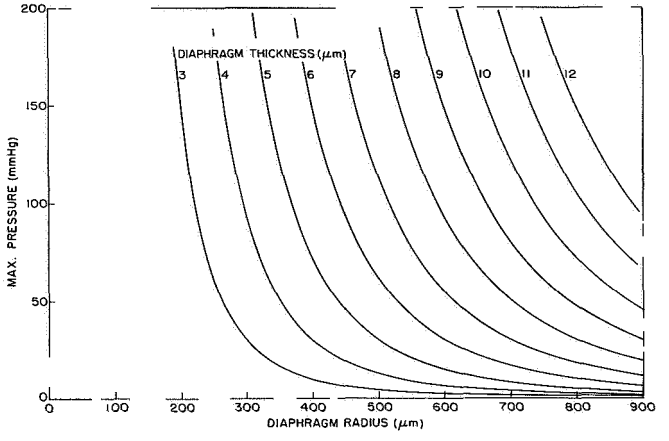

Fig 3 Maximum pressure for linearity as a function of diaphragm radius for a clamped silicon diaphragm The diaphragm thickness is used as a parameter and $(w_c/h) < 0.4$ is taken as the maximum deflection limit

distance from the center r by the expression *[2]*, [3]

$$\sigma_r = \frac{39}{8h^2}\left[a^2(1+\nu) - r^2(3+\nu)\right]$$

$$\sigma_t = \frac{39}{8h^2}\left[a^2(1+\nu) \quad r^2(1+3\nu)\right] \tag{1}$$

Fig. *2* shows this stress pattern as a function of the distance from the center of the diaphragm. This linear relation between the applied pressure and the stress on the diaphragm is only valid for deflections that are small compared to the thickness of the diaphragm. This implies that no longitudinal stress exists at the neutral plane of the diaphragm.

The magnitude of the deflection at the center of the diaphragm is [3], [4]

$$w_c = \frac{3qa^4(1-\nu^2)}{16Eh^3}, \qquad E \text{ is Young's modulus.}$$

Fig. *3* shows the relation between the maximum allowable pressure and the diaphragm radius using the diaphragm thickness as a parameter, while $w_c/h < 0.4$ is taken as the limiting value (ensuring linearity to better than 1 percent). Exceeding these maximum pressures, a nonlinear relation between applied pressure and stress on the diaphragm will be observed.

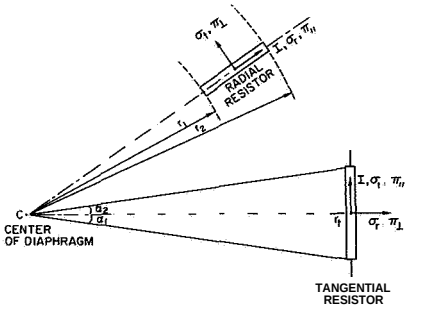

Fig. 4 Stresses and piezoresistive coefficients of tangential and radial resistors.

For a piezoresistor subjected to parallel and perpendicular stresses the relationship between the fractional change in resistance and the perpendicular and parallel stress component **is**

$$\frac{\Delta R}{R} = \pi_{\|}\sigma_{\|} + \pi_{\perp}\sigma_{\perp} \tag{2}$$

where $\pi_{\|}$ and $\pi_{\perp}$ are the parallel and perpendicular piezoresis, tive coefficients, respectively For tangentially and radially oriented piezoresistors (Fig. *4)* on a circular diaphragm whose radius is large compared with the resistor dimensions, this fractional change in resistance can be expressed as follows

tangential resistors.

$$\left(\frac{\Delta R}{R}\right)_t = \pi_{\|}\sigma_t + \pi_{\perp}\sigma_r$$

radial resistors

$$\left(\frac{\Delta R}{R}\right)_r = \pi_{\|}\sigma_r + \pi_{\perp}\sigma_t \tag{3}$$

The expressions for the parallel and perpendicular piezoresistive coefficients are *[4]* **as** follows

n-type

$$\pi_{\|} = \pi_{11}\left[1 \quad 3(l_1^2m_1^2 + l_1^2n_1^2 + m_1^2n_1^2)\right]$$
$$\pi_{\perp} = \pi_{11}\left[-\frac{1}{2} + \frac{3}{2}(l_1^2l_2^2 + m_1^2m_2^2 + n_1^2n_2^2)\right]$$

p-type

$$\pi_{\|} = 2\pi_{44}(l_1^2m_1^2 \; l_1^2n_1^2 + m_1^2n_1^2)$$
$$\pi_{\perp} = \pi_{44}(l_1^2l_2^2 + m_1^2m_2^2 + n_1^2n_2^2) \tag{4}$$

where l_1, m_1, and n_1 are the direction cosines of a vector parallel to the resistors, with respect to the crystallographic axes, and l_2, m_2, and n_2 are the direction cosines of a vector perpendicular to the resistors, also with respect to the crystal. lographic axes. π_{11} and π_{44} are the dominant piezoresistive coefficients in n- and p-type piezoresistors, respectively

Combining (1), (3), and (4), we can calculate the fractional change in piezoresistors that are diffused on a (100) oriented diaphragm and directed in the major axes. For n-type

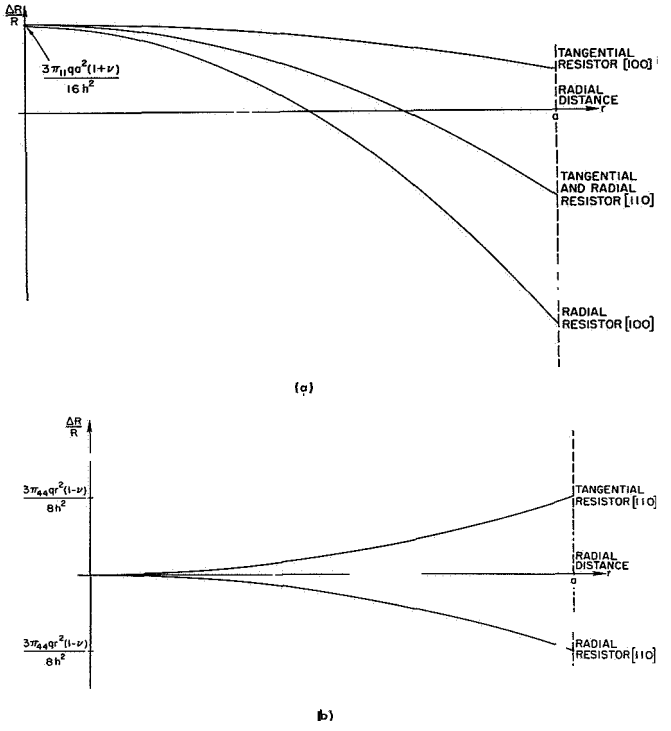

Fig. 5 (a) Fractional resistance change $\Delta R/R$ versus radial distance r for tangential and radial n-type diffused resistors in different crystallographic directions in the (100) plane (b) Fractional resistance change $\Delta R/R$ versus radial distance r for tangential and radial p-type diffused resistors in the [110] direction on the (100) plane

resistors in the [100] and [110] directions, the expressions are as follows.

[100]

$$\left(\frac{\Delta R}{R}\right)_t = \pi_{11}\,\frac{3q}{16h^2}\,[a^2(1+\nu)+r^2(1-5\nu)]$$

$$\left(\frac{\Delta R}{R}\right)_r = \pi_{11}\,\frac{3q}{16h^2}\,[a^2(1+\nu)+r^2(5-\nu)]$$

[110]

$$\left(\frac{\Delta R}{R}\right)_r = \left(\frac{\Delta R}{R}\right)_t = \pi_{11}\,\frac{3q}{16h^2}\,[a^2(1+\nu)-r^2(2+2\nu)] \qquad (5)$$

For p-type resistors oriented in the [100] direction, $\pi_{\parallel}$ and $\pi_{\perp}$ are both zero, while for the [110] direction they are as follows:

[110]

$$\left(\frac{\Delta R}{R}\right)_r = -\left(\frac{\Delta R}{R}\right)_t = -7744\,\frac{3qr^2}{8h^2}\,(1-\nu). \qquad (6)$$

These functions are plotted in Fig. 5(a) and (b), respectively

From these figures we conclude that, for n-type resistors diffused into the **(100)** plane, the best arrangement to get four active resistors in a bridge is to have two resistors, either tangential or radial, near the center of the diaphragm in either the [100] or [110] direction and two radial resistors in the [100] direction far from the center

For a bridge containing four active p-type resistors, the best combination would be two radial and two tangential resistors in the [110] direction, all located at the rim of the diaphragm.

For practical resistors diffused on a circular diaphragm, averaging techniques must be used to calculate the fractional change due to an applied pressure, since piezoresistors occupy a finite area on the diaphragm. The appropriate averaging integrals have been described in the literature **[2], [4]**

Resistor Value

The choice of the value of the piezoresistors must represent a compromise among several conflicting requirements. The pressure sensitivity of a bridge containing four active piezoresistors is proportional to the sheet resistivity and the supply voltage. The temperature stability, on the other hand, is inversely proportional to the sheet resistivity and the supply voltage so that the requirement for good temperature stability conflicts with the requirement for large pressure sensitivity

Using appropriate temperature-compensation circuits, most of the temperature drift can be eliminated within a certain temperature span so that a high sheet resistivity and supply voltage can give distinct advantages The upper limit of the supply voltage is set by safety and maximum dissipation considerations, this limit is usually between **6** and 15 V The upper limit of the sheet resistivity is determined by such practical considerations as whether or not signal-processing circuitry is going to be integrated on the chip P-type resistors are usually processed using the base diffusion schedule, which yields a sheet resistivity of about **100** Ω/square For a given resistance value, the average piezoresistive coefficient of a resistor tends to increase with smaller size The minimum size of a resistor is determined by the available photolithographic resolution and the sheet resistivity For ultraminiature pressure sensors where no additional signal-processing circuitry is planned on the chip, a sheet resistivity higher than **100** Ω/square is desirable In this case, for a certain limit in photolithographic resolution, the size of the resistors can be minimized.

FABRICATION

Resistor Formation

The starting material used for the fabrication of the pressure sensors is n-type, 50–75 μm thick, (100)-oriented silicon wafers They are supplied with one side of the wafer polished, and both sides covered with silicon dioxide (Monothin, Monsanto Co., St. Louis, Mo).

The first processing step involves the stripping of the onginal oxide of the wafers and regrowing it at a temperature of **1100°C** to a thickness of 7000 Å This step is important if a good control of the temperature coefficient of the finished pressure sensor is needed, since, as will be shown later, the temperature coefficient is mostly determined by the characteristics of this oxide This oxide is used as a mask for the resistor and substrate contact diffusions and also as a mask during the diaphragm etching step

To facilitate the photolithography of related patterns on the front and back side of the wafer, alignment marks are photo-

engraved on both sides of the wafer using a special jig, and succeeding masks are then aligned with respect to these marks. The alignment marks are aligned with flats on the wafer derived by cleaving the wafer along the [110] crystallographic directions [4]

To make the fabrication as compatible as possible with standard bipolar IC processing, the p-resistors are diffused according to a standard base diffusion schedule, resulting in a sheet resistivity of close to 100 Ω/square This schedule yields resistors with a high piezoresistive coefficient and should also make possible the incorporation of on-chip signal processing at a later stage in sensor development Substrate contacts (doped n^+) are formed using a standard emitter diffusion schedule

After opening the contact holes and removing the photoresist, nickel is then evaporated over the entire wafer to a thickness of approximately 1500 Å Again using photolithography, contact pads are selectively electroplated either with gold or nickel, depending whether the output wires are going to be bonded or soldered on the pads The excess nickel is then etched away, and the wafers are ready for the diaphragm etching step.

Diaphragm Formation

There are several ways of constructing the silicon diaphragm Due to the brittleness of silicon, handling problems are encountered with thin diaphragms so that an ideal construction would have a thin silicon diaphragm surrounded by a thicker supporting rim of silicon There are several potential methods of achieving this goal, such as the spark gap erosion technique [5], electrochemical etching [6], and selective etching. Large-area thick diaphragms of approximately 20 μm thickness have been constructed using the $HF\text{-}HNO_3$ isotropic selective etch technique, using black wax or silicon dioxide as a protection mask, The rounding off of the edges in this kind of etching can be avoided for large-area diaphragms (1-in diam diaphragms for silicon vidicon targets) using either careful agitation or gas bubbling [7] Diaphragm thickness control is done either by monitoring the transmitted light through the diaphragm or the etching time The first method of monitoring is practical only for large-area diaphragms, while etching time monitoring needs a careful control of etch rate by controlling the etch temperature and the etch composition. For thin diaphragms of the order of 5 μm, problems of control of these parameters can considerably lower the processing yield. Since ultimately the circular chips must be separated from the wafer, a final separation etch must be introduced that creates the problem of finding the appropriate metals for the contact pads that can withstand this final etch step

The method we are using to make our diaphragms utilizes an anisotropic etch Several etchants of this type are available, such as hydrazine [8], pyracatechol [9], and potassium hydroxide [10] The etch we are using is the last named, which is relatively inexpensive and easy to handle, while masking is easily accomplished using thermally grown silicon dioxide. To circumvent any lack of reproducibility in final thickness due

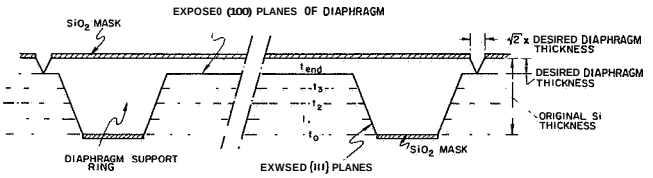

Fig. 6. Formation of thin silicon diaphragms with a supporting rim. The chip separation etch, which is done together with the diaphragm formation etch, is used as a thickness indicator

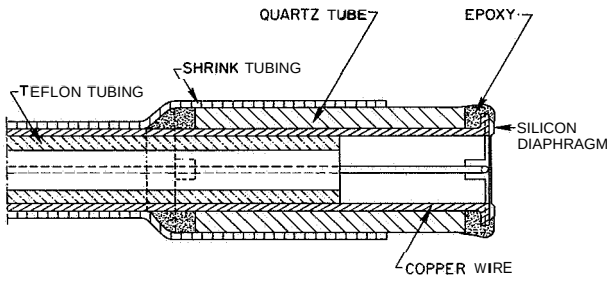

Fig. 7 Catheter-tip mounting of the large (1.6-mm OD) pressure sensor

to different etch rates and starting wafer thicknesses, a diaphragm thickness monitoring scheme has been developed. A cross section of the transducer structure during the diaphragm etching process is shown in Fig. 6 A narrow slot opening is made in the silicon dioxide etch mask on the front surface of the wafer to define the boundary of the desired transducer chip The width of this slot in the upper etch mask is set equal to 1.4 times the desired diaphragm thickness. As the etching proceeds from the back surface to define the diaphragm, it also etches a groove in the upper surface The sides of this groove correspond to the (111) crystallographic planes. After a few minutes, the groove bottoms out to form a V, after which time no (100) surface is exposed. Since the etch rate in the [100] direction is about 100 times faster than in the [111] direction, the etch slows down considerably on the front side of the wafer and proceeds only from the back side The depth of the groove corresponds to the final diaphragm thickness. As the diaphragm reaches this desired thickness, the transducer separates from the wafer This separation is easily observed and an etch quenching step can then be initiated. Using this technique, we need only to watch for the moment of die separation at which time the diaphragm has reached the required thickness irrespective of the original wafer thickness and the etch rate Etching temperatures between 70 and 80°C are satisfactory and yield an etch rate of about 0.5 μm/min in the (100) direction.

Mounting of the Pressure-Sensitive Chips

For intravascular cardiac pressure measurements, the chips must be mounted on the tip of the catheter Fig. 7 shows a diagram of a cross section of the catheter-tip mounting of large (1.6-mm chip diam) pressure sensors. Four insulated copper wires are threaded through the quartz tube and held in place by the Teflon tube that also acts as a reference pressure conduit The four wires are positioned approximately 90" apart

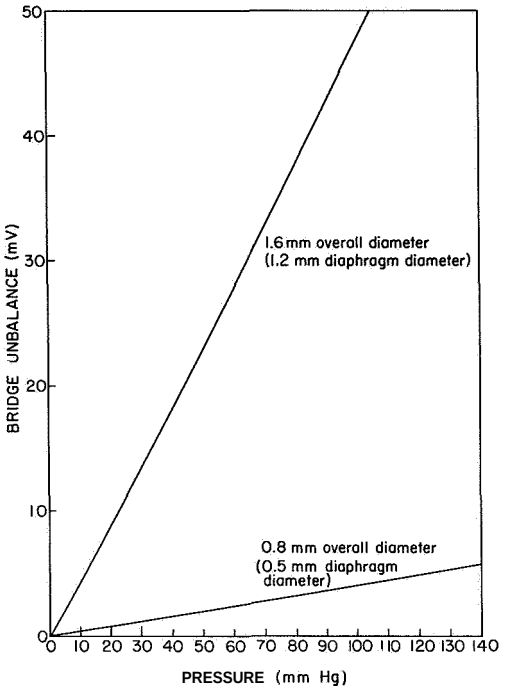

Fig. 8 Pressure sensitivity of pressure sensors with different diaphragm diameters.

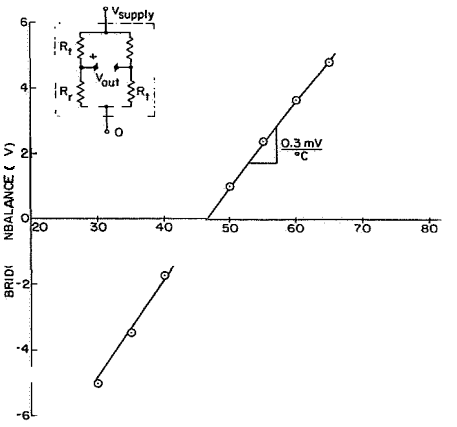

Fig. 9 Temperature drift of an unmounted pressure sensor

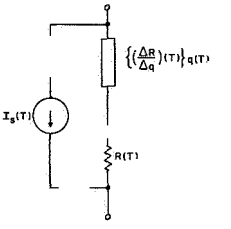

Fig. 10. DC model of a piezoresistor

so that they align with the four contact pads on the pressure-sensitive chip After applying emulsified solder to the wires, they are brought into contact with the pads and the whole structure is heated to melt the solder The space between the chip and the quartz tube is then filled with epoxy

The mounting of the small (0.8-mm diam) pressure sensors is done with a slight modification of the technique used for mounting the larger sensors. Instead of using Teflon for positioning the four copper wires, they are twisted together and epoxied at one end

ELECTRICAL CHARACTERIZATION

Bridge Unbalance Voltage versus Pressure

Fig. 8 shows the piezoresistor–bridge unbalance voltage as a function of applied pressure for two pressure-sensitive chips of 1 2- and 0.5-mm diaphragm diam, respectively In both cases, the diaphragm thickness is 7 μm. A supply voltage of **6** V was used for the experiments so that the pressure sensitivities of the pressure sensors are, respectively, 83 and 14 **μV/V** supply/mmHg. Some nonlinearity is observed in the pressure sensitivity of the 1 2-mm **diam** pressure sensor due to the nonlinear relation between the applied pressure and the stress on the diaphragm

The high sensitivities realized for these sensors permit pressure variations as small **as** 0.1 and 1 mmHg to be resolved with the 1 2- and 0.5-mm **diam** diaphragms, respectively Even with these thin diaphragms, the pressure sensitivities of all sensors realized from a processing run are usually within 15 percent of the average value, with the variations attributed to small differences in diaphragm thickness from sensor to sensor For a given device, any observed variations in the output signal at constant pressure can be attributed to ambient temperature changes as discussed below We have not observed any changes in sensitivity due to repeated diaphragm flexing. Once these sensors are calibrated and compensated for temperature variations, they are accurate to within 1 mmHg or better for dc or ac[1] pressures ranging from the minimum resolvable to at least 150 mmHg.

From the pressure sensitivity and the known values of diaphragm diameter and thickness, we can calculate the piezoresistive coefficient of the diffused p-type resistors for our value of sheet resistivity Substituting the known values into the following equation

$$\frac{V_{\text{out}}}{V_{\text{supply}}} = \frac{1}{2}\left\{\left(\frac{\Delta R}{R}\right)_r - \left(\frac{\Delta R}{R}\right)_t\right\}$$

and equating it with the measured sensitivities, we find the value of $\pi_{44} = 75 \times 10^{-12}$ cm^2 dyn^{-1} This value of π_{44} is in agreement with the published value for the resistivity used.

Temperature Sensitivity of Diffused Piezoresistors

The change in the bridge unbalance voltage as a function of temperature, for an unmounted pressure sensor with no applied pressure, is shown in Fig. 9 This temperature coefficient corresponds to 0.3 mV/°C for a **6-V** supply voltage (equivalent to 0.6 mmHg/°C).

[1] **The frequency response of these transducers is more than adequate for biomedical applications. Although detailed frequency measurements have not been made above 10 kHz, the first calculated diaphragm resonance is at about 60 kHz for the 1.2-mm diaphragm, and is considerably higher for the smaller sensor**

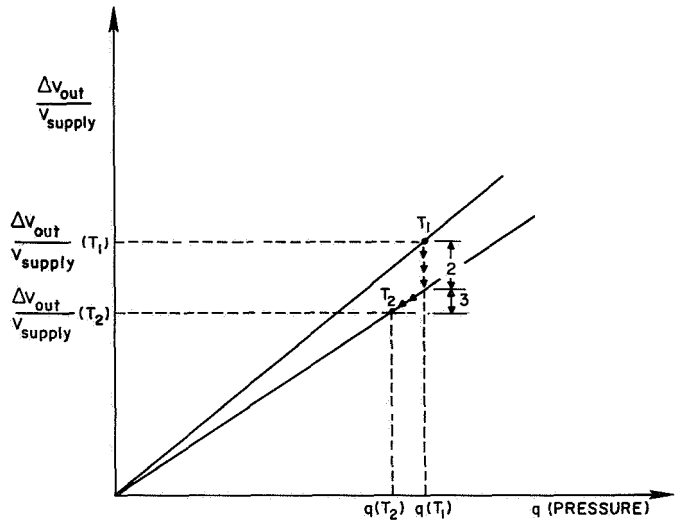

Fig. 11 Graphical representation of the temperature behavior **of** a diffused piezoresistive pressure sensor

A dc model of a piezoresistor is shown in Fig. 10. The total drift is caused by the combined effects of temperature on the individual members of the equivalent circuit. These effects are as follows.

1) $R(T)$ is the temperature-dependent value of the unstressed piezoresistor at a particular temperature

2) The pressure sensitivity of the piezoresistor is expressed by the term $(\Delta R/\Delta q)(T)$, which is also temperature dependent

3) $q(T)$ is the effective pressure on the diaphragm that consists of two terms, namely, the applied pressure on the diaphragm and additional stresses sensed on the diaphragm due to the silicon dioxide layer on the silicon diaphragm Since the oxide layer is grown at an elevated temperature, a temperature-dependent residual stress is present at room temperature due to the difference in thermal expansion coefficients between the silicon and the overlying silicon dioxide.

4) $I_s(T)$ is the temperature-dependent leakage current between the reverse biased piezoresistors and the substrate, it is actually a distributed current source. This leakage current is usually negligible for properly processed wafers.

Another source of temperature effect, which is not considered in this analysis, could arise in a mounted device due to the additional stress caused by a mismatch in the thermal expansion coefficient between the pressure sensor and its housing.

The temperature coefficient of the resistivity (component 1) is due to the temperature dependence of carrier mobility This temperature coefficient has a value of about 1000 ppm/°C for boron-doped resistors with a resistivity of 100 Ω/square. Since the coefficients of **all** the resistors have the same sign, the temperature coefficient of the bridge unbalance is determined by differences in the temperature coefficients of the radial and tangential resistors. These differences, caused by the differing surface concentrations of the individual resistors, are typically of the order of 0.5 percent The expected variations of the bridge unbalance due to this effect then are of the order of 5 ppm/°C, or equivalent to less than 0 1 mmHg/°C For carefully executed **IC** processing of the sensors, this part of the total temperature coefficient can be neglected

A graphical representation of the temperature effects due to oxide stress and the temperature dependence of the piezoresistive coefficient is shown in Fig. 11 with no applied pressure on the diaphragm. The total change of V_{out}, for a temperature variation from T_1 to T_2 $(T_2 > T_1)$, is composed of components 2 and 3. Component 2 is caused by the change in the piezoresistive coefficient due to temperature and component 3 by the temperature effect on the residual stress on the silicon–silicon dioxide interface. The effective pressure on the diaphragm changes from $4(T_1)$ to $q(T_2)$.

The value of the residual pressure on the diaphragm due to the oxide has been measured by comparing the difference in bridge unbalance for a sensor before and after the diaphragm etch For oxides grown at 1100°C and with a thickness of about 5000 Å, the measured room temperature stress on the diaphragm due to this oxide is equivalent to 70 mmHg applied pressure The residual stress at the silicon–silicon dioxide interface, which shows itself as a slight bowing of the diaphragm, can be expressed as [12]

$$\sigma = C(\alpha_{Si} \quad \alpha_{SiO_2})(T_2 - T_1)$$

where C is a structural constant with the dimension of stress, α_{Si} and α_{SiO_2} are, respectively, the expansion coefficients of silicon $(3\ 7 \times 10^{-6}/°C)$ and silicon dioxide $(1.6 \times 10^{-6}/°C)$, and $(T_2 \quad T_1)$ is the temperature range for the stress buildup Since both silicon and silicon dioxide are soft at 1100°C, we cannot use this value for T_2 Jaccodyne [13], in his stress analysis of structures consisting of a silicon beam coated with a thermally grown silicon dioxide layer, uses the value of 800°C as the temperature limit of plasticity Using this value as T_2, the temperature Coefficient of this residual stress is also equivalent to less than 0.1 mmHg/°C From these data we conclude that the temperature coefficient of the unmounted pressure sensor is dominated by the temperature coefficient of the piezoresistive coefficient (component 2). This conclusion is in agreement with the predictable uniform direction of the shift of the bridge unbalance with temperature for different sensors.

In the case of a mounted pressure sensor, any mismatch in the expansion coefficient between the sensor and the mounting will also be mterpreted as a residual stress by the diaphragm and reflect into the temperature coefficient of the packaged transducer. This mismatch in the temperature expansion coefficient can dominate the final temperature drift of the finished transducer The temperature drift of a catheter-mounted pressure sensor is much less predictable than that of an unmounted one For a typical mounted sensor, this drift is approximately 5 mmHg/°C, which is mostly due to the difference in the temperature expansion coefficient of the materials used for the mounting and the stresses introduced on the diaphragm during the mounting. This temperature drift is excessive for most biomedical applications and a temperature-compensation scheme must be devised.

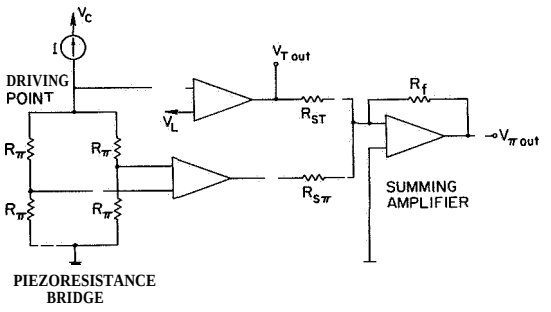

Fig. 12 Temperature-compensationcircuit

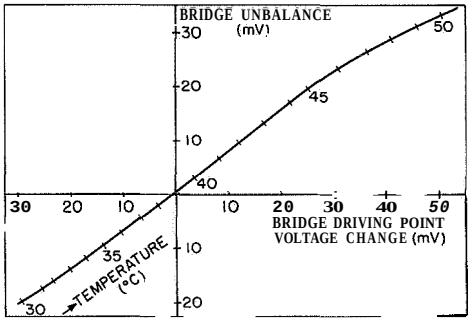

Fig. 13 Relationship between the change in bridge unbalance and the change in bridge driving-point voltage as a function of temperature for a typical catheter-tip-mountedpressure sensor

Temperature Compensation

There are several schemes available to compensate for the temperature drift of the pressure sensor [11] The compensation scheme shown in Fig. 12 uses active circuits external to the catheter to minimize the temperature drift By driving the bridge through a current source, a temperature-dependent signal that is pressure independent can be obtained from the driving point and used to compensate for the temperature drift of the bridge unbalance. An added benefit of this circuit is the availability of a temperature-dependent signal for measuring the temperature of the biological system.

For a typical catheter-tip-mounted pressure sensor, the ratio of R_{st} and $R_{s\pi}$ can be found from the curve relating the change in bridge driving-point voltage to the change in bridge unbalance voltage for the temperature range of interest, as shown in Fig. 13 In practice, this ratio is mostly determined by the effect of temperature on resistivity, as reflected on the driving-point voltage, and by the effect of temperature on the piezoresistive coefficient and other temperature stresses introduced by the packaging, as reflected on the bridge unbalance voltage

A pressure-sensitivity curve of a temperature-compensated pressure transducer is shown in Fig. 14 for three different temperatures. The compensation is essentially perfect between 33 and 39°C, while between 39 and 43°C the temperature drift is approximately 1 mmHg/°C Due to the unpredictable nature of the temperature drift of the mounted devices, each device must be compensated individually

BIOMEDICAL EVALUATION

The pressure sensors have been evaluated by using them to measure the blood pressure in the circulatory system of dogs. After undergoing a chemical sterilization step by dipping them

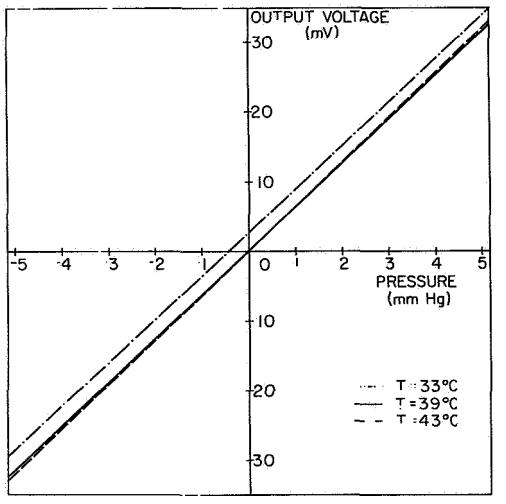

Fig. 14 Pressure sensitivity of a temperature-compensated pressure sensor

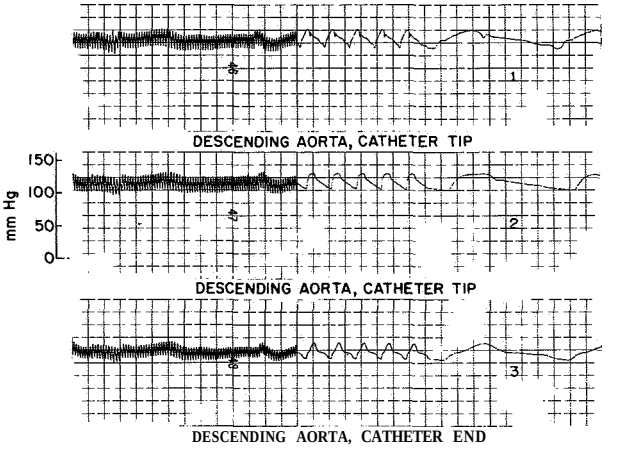

Fig. 15 Recordings of the blood pressure inside the descending aorta of a dog (See text for an explanation of the different traces.)

for a few minutes in a Gerticide solution, they are then in. serted into the left descending aorta of an anesthetized dog, and afterwards guided to the desired upstream location using a fluoroscope Fig. 15 shows a recording of the blood pressure inside the descending aorta of a dog using three different pressure sensors. Traces 1 and 3 were both measured near the aortic valve using commercially available pressure sensors. Trace 1 was obtained with a catheter-tip-mounted pressure sensor (2.5-mm OD), while trace 3 utilizes a sensor that was mounted at the end of a catheter outside the dog. Trace 2 was measured with our large (2.2-mm OD) pressure sensor, located approximately 20 cm from the aortic valve It is seen from the traces that the fidelity of the two catheter-tip-mounted pressure sensors is much better than that of the catheter-end. mounted one, which is characterized by a slight ringing of the pressure waveform due to the pressure wave propagation char. acteristics within the long catheter

Fig. 16 shows a recording of the blood pressure in the left ventricle of a dog using our small catheter-tip-mounted pressure sensor This pressure sensor has an overall diameter of 0.9 mm. The sensor was brought into the left ventricle by in. serting it through the inner bore of a larger catheter This

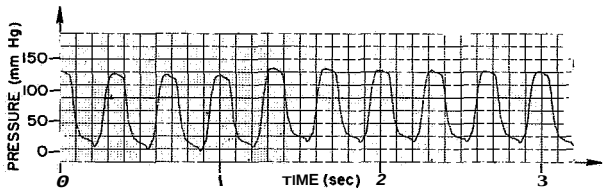

Fig. 16. Recording of the blood pressure in the left ventricle of a dog using the 0.9-mm OD catheter-tip-mounted sensor

large catheter (3-mm OD and 1 1-mm bore) was brought into the left ventricle with the help of a guide wire that was later taken out and replaced by our pressure sensor

Since extensive evaluation of the pressure sensors using simulated conditions had been done prior to actual *in vivo* use, the main purpose of the *in vivo* measurements has been to determine if the catheter-mounted device could withstand rough treatment during insertion into the dog and whether any reaction does occur between the sensor and the blood From the data obtained so far the sensors seem to be sturdy enough to survive the insertion and no noticeable reaction has occured either with the silicon or the epoxy sealant during acute measurements (90-min duration) in the cardiovascular system of a dog. The recessed location of the diaphragm. due to the thick protection nm, definitely helps in preventing direct contact of the thin silicon diaphragm with the arterial wall during insertion, thus minimizing the possibility of diaphragm breakage

CONCLUSION

A piezoresistive pressure sensor for biomedical instrumentation has been developed that allows outer diameters of as small as 0.8 mm so that insertion of the finished sensor can be done through a catheter that has been guided to the desired location using a guide wire An intrinsic sensitivity of 14 μV/V supply/mmHg is made possible through a technique for reliably making 5-pm thick silicon diaphragms surrounded by a thick rim This technique was developed during the course of investigation of these miniature pressure transducers. The possibility of using IC techniques to batch fabricate these pressure sensors with a high yield makes the realization of a cheap disposable cardiovascular pressure transducer a real possibility

In order to utilize the high piezoresistive coefficient of lightly doped piezoresistors. the temperature coefficient of the piezoresistors has been investigated It was shown that the temperature stability of these piezoresistorsis dominated by the temperature dependence of the piezoresistive coefficient A temperature-compensation circuit that does not diminish the intrinsic sensitivity of the sensor has been developed, this circuit provides a temperature-dependent signal that is pressure independent for compensating the temperature-dependent part of the sensor output

Acute intravascular testing of the catheter-tip-mounted sensors has been conducted in dogs with satisfactory results. The sensors were sturdy enough to survive the insertion into the heart Although the possibility of breaking the diaphragm during normal use is remote, investigation should be conducted into the possible effects of this and safeguards developed against microshock

The possibility of introducing integral signal-processing circuitry on the chip of the larger pressure sensors is also worth pursuing. A circuit that could minimize the number of leads coming from the chip would be desirable, since it will make the mounting of the sensors on the tip of a catheter much easier

Other techniques for compensating the temperature drift of the sensors should also be investigated. This might be achieved by manipulating the temperature characteristics of the conduction mechanism in the semiconductor by techniques such as ion implantation.

Although a method has been developed for batch fabricating the miniature pressure sensors, further development of the packaging is needed. This is especially true if the pressure sensors are going to be chronically implanted The interesting possibility of using the package as part of the temperature-compensation scheme should not be overlooked. By selecting the expansion coefficient of the package smaller than that of silicon, much of the temperature drift might be eliminated.

ACKNOWLEDGMENT

The authors wish to thank N. Tombs, J Dimeff, and B Beam, all of the NASA Ames Research Center, for their cooperation and guidance during this program They also wish to thank Dr H Sandler, also of NASA-Ames, for his assistance in the *in vivo* evaluation of the sensors, and E D. Nielsen, Stanford University, for his contributions.

REFERENCES

[1] J J Wortman and L K. Monteith, "Semiconductor mechanical sensors," *IEEE Trans. Electron Devices (Special Issue on Solid State Sensors).* vol. ED-16. pp. 855–860, Oct 1969
[2] O. N Tufte *et al.*, "Silicon diffused-element piezoresistive diaphragms," *J Appl. Phys.* vol. 33, pp 3322–3327, 1962
[3] S. Timoshenko, *Theory of Plates and Shells.* New York McGraw-Hill, 1940.
[4] Samaun, "IC piezoresistive pressure sensor for biomedical instrumentation," Ph.D dissertation, Dep. Elec Eng., Stanford Univ., Stanford, Calif., Aug. 1971
[5] A C M Gieles, "Subminiature silicon pressure transducer," in 1969 *Int. Solid State Circuits Conf. ,Dig. Tech. Papers,* p. 108
[6] M. J J Theunissen *et al.*. "Application of preferential electrochemical etching of silicon to semiconductor device technology." *J. Electrochem. Soc.* vol. 117, pp 959–965, July 1970.
[7] A. I Stoller *et al.*. "A new technique for etch thinning silicon wafers," RCA *Rev.,* vol. 31. pp. 265–270. June 1970.
[8] D. B. Lee, "Anistropic etching in silicon," *J. Appl. Phys.,* vol 40, pp. 4569–4574. Oct. 1969
[9] J C Greenwood, "Ethylene diamine-cathecol-water mixture shows preferential etching of p-n junctions," *J. Electrochem Soc. vol.* 116, pp 1325–1326, Sept. 1969
[10] A I Stoller, "The etching of deep vertical-walled patterns in silicon," *RCA Rev.*. vol 31 pp. 271–275, June 1970
[11] Dean and Douglas, *Semiconductor Strain Gages,* Instrum. Soc Amer 1962
[12] S. Timoshenko, "Analysis of bimetal thermostats," *J Opt Soc Amer.,* vol. 11 pp. 233–255. Sept 1925
[13] R J Jaccodyne *et al.*, "Measurements of strains at $Si\text{-}SiO_2$ interface." *J. Appl. Phys.* vol. 37 pp 2429–2434. May 1966